Available online at www.sciencedirect.com
ScienceDirect
Developmental Biology 304 (2007) 208–220
DEVELOPMENTAL BIOLOGY
www.elsevier.com/locate/ydbio

Defects in brain patterning and head morphogenesis in the mouse mutant *Fused toes*

Isabelle Anselme [a,1], Christine Laclef [a,1], Magali Lanaud [a,1], Ulrich Rüther [b], Sylvie Schneider-Maunoury [a,*]

[a] *Biologie du Développement, CNRS UMR7622, Université Pierre et Marie Curie, 9 Quai Saint-Bernard, 75252 Paris Cedex 05, France*
[b] *Institute for Animal Developmental and Molecular Biology, University of Düsseldorf, Universitätsstr. 1, 40225 Düsseldorf, Germany*

Received for publication 30 May 2006; revised 17 November 2006; accepted 12 December 2006
Available online 15 December 2006

Abstract

During vertebrate development, brain patterning and head morphogenesis are tightly coordinated. In this paper, we study these processes in the mouse mutant *Fused toes* (*Ft*), which presents severe head defects at midgestation. The *Ft* line carries a 1.6-Mb deletion on chromosome 8. This deletion eliminates six genes, three members of the *Iroquois* gene family, *Irx3*, *Irx5* and *Irx6*, which form the *IrxB* cluster, and three other genes of unknown function, *Fts*, *Ftm* and *Fto*. We show that in *Ft/Ft* embryos, both anteroposterior and dorsoventral patterning of the brain are affected. As soon as the beginning of somitogenesis, the forebrain is expanded caudally and the midbrain is reduced. Within the expanded forebrain, the most dorsomedial (medial pallium) and ventral (hypothalamus) regions are severely reduced or absent. Morphogenesis of the forebrain and optic vesicles is strongly perturbed, leading to reduction of the eyes and delayed or absence of neural tube closure. Finally, facial structures are hypoplastic. Given the diversity, localisation and nature of the defects, we propose that some of them are caused by the elimination of the *IrxB* cluster, while others result from the loss of one or several of the *Fts*, *Ftm* and *Fto* genes.

Keywords: *Fused toes*; *Irx*; Craniofacial; Brain patterning; *Ftm*; *Fts*; *Fto*; Midbrain; Forebrain; Telencephalon

Introduction

The generation of functional diversity in the vertebrate brain requires the progressive subdivision of the neural tube, the prospective central nervous system (CNS), into distinct domains along its anteroposterior (AP) and dorsoventral (DV) axes. Brain patterning begins during gastrulation, with the formation of the neural plate in the dorsal ectoderm. In mouse embryos, adjacent tissues such as the node and the anterior visceral endoderm send signals that subdivide the neural plate into distinct gene expression domains (for review, Ang and Behringer, 2002; Robb and Tam, 2004). Later, cross-regulatory interactions between transcription factors expressed in overlapping or adjacent domains, combined with the action of secondary signalling centres that form at boundaries between these domains, act to further pattern the neural tissue (for review, Kiecker and Lumsden, 2005; Rhinn and Brand, 2001; Wilson and Houart, 2004). Several of these signalling centres have been described extensively, such as the floor plate and roof plate, the anterior neural ridge (ANR), the midbrain–hindbrain boundary (MHB), the *zona limitans intrathalamica* (ZLI), and rhombomere boundaries. They organise morphogenesis and cell fate in the adjacent neural domains (Kiecker and Lumsden, 2005; Rhinn and Brand, 2001; Wilson and Houart, 2004).

Brain patterning and craniofacial morphogenesis are tightly linked processes. These two structures arise in close vicinity. The anterior border of the neural plate gives rise to the ectoderm of the face and to the nasal ectoderm and olfactory placodes. More caudally, the lateral edge of the neural plate gives rise to the cranial neural crest, which migrates into the periphery to form bones, cartilages and connective tissues of the face and

* Corresponding author. Fax: +33 1 44 27 34 45.
E-mail address: sylvie.schneider-maunoury@snv.jussieu.fr (S. Schneider-Maunoury).
[1] These authors have contributed equally to the work reported in this paper.

0012-1606/$ - see front matter © 2006 Elsevier Inc. All rights reserved.
doi:10.1016/j.ydbio.2006.12.025

neck, as well as peripheral nervous system (PNS) neurons and glia (Depew et al., 2002; Le Douarin and Kalcheim, 1999). Neural crest from the posterior diencephalon and midbrain migrates to the frontonasal and periocular regions, and to the first branchial arch (BA1). Hindbrain neural crest cells migrate in three streams into the branchial arches, and form the jaw, ear and neck structures (Depew et al., 2002; Le Douarin and Kalcheim, 1999). As a consequence of their close apposition, brain and craniofacial structures share several developmental processes. First, common signalling centres, such as the ANR, the prechordal plate, and the endoderm of the foregut, are involved in brain and face formation (Couly et al., 2002; Schneider et al., 2001; Shimamura and Rubenstein, 1997). Second, the forebrain acts as a structural support for facial development, as exemplified by the human condition holoprosencephaly (Marcucio et al., 2005; Muenke and Cohen, 2000). Finally, these two structures depend on each other for their morphogenesis (Creuzet et al., 2004; Marcucio et al., 2005; Schneider et al., 2001).

In this paper we study a mouse mutant, *Fused toes* (*Ft*), which, at the homozygous state, presents severe brain and craniofacial defects. The name of this autosomal dominant mutation is based on the phenotype of the heterozygous animals: a fusion of digits 1 to 4 of the forelimbs (Heymer and Rüther, 1999; van der Hoeven et al., 1994). Homozygous *Ft* embryos die between 9.5 and 13.5 days post-coitum (dpc) and present many abnormalities. The limbs show AP and DV polydactyly and distal truncations (Grotewold and Rüther, 2002). Left–right asymmetry of heart looping and embryo turning is randomised (Heymer et al., 1997). The floor plate forms but is not maintained, and DV patterning of the spinal cord is perturbed (Götz et al., 2005).

The *Fused toes* mutation is a 1.6-Mb deletion on mouse chromosome 8. This deletion eliminates six genes: three members of the *Iroquois* gene family, *Irx3*, *Irx5* and *Irx6*, which form the *IrxB* cluster, and three other genes of unknown function, *Fts*, *Ftm* and *Fto* (Peters et al., 2002). *Iroquois* genes code for homeodomain transcription factors highly conserved from *Drosophila* to mammals. They are characterised by a homeodomain containing a 3-amino-acid loop extension (TALE), and a conserved 13-amino-acid motif called the Irobox (for review, Cavodeassi et al., 2001; Gomez-Skarmeta and Modolell, 2002). Several functions of the vertebrate *Iroquois* genes have been identified, mainly by overexpression studies in Xenopus, zebrafish and chicken. They include organizer formation, neural plate formation and patterning, sensory placode formation, and heart formation and function (for review, Cavodeassi et al., 2001; Gomez-Skarmeta and Modolell, 2002). In the central nervous system, *Iroquois* genes are involved in positioning boundaries within the diencephalon (Kobayashi et al., 2002) and hindbrain (Lecaudey et al., 2004), in specifying interneuron identity in the chick spinal cord (Briscoe et al., 2000; Novitch et al., 2001) and also in the formation of brain territories such as the mid–hindbrain region (Itoh et al., 2002) and the cerebellum (Matsumoto et al., 2004). In the mouse, the function of the *IrxB* cluster in the brain has not been investigated. Inactivation of *Irx5* in the mouse has shown the requirement for this gene in heart physiology (Costantini et al., 2005). For *Irx3* and *Irx6*, no functional study has been reported so far in this species. Considering the probable functional redundancy within *Iroquois* clusters, the *Ft* mutation is a good model for the functional analysis of this transcription factor family. In this paper we analyse early steps of brain and craniofacial development in *Ft* mice.

Materials and methods

Mice

Ft mice have been described previously (van der Hoeven et al., 1994). They were maintained under two distinct genetic backgrounds: an inbred C3H background and a mixed C57Bl6/DBA2 background. We did not see any significant difference between the two backgrounds in the strength of the phenotypes observed with molecular markers. The morphology of the brain was variable between homozygous individuals, even in an inbred background. Adult heterozygote carriers were identified by their digit fusion in the forelimb. Embryos issued from timed heterozygous matings were isolated at the desired stages, and genotypes as described previously (Götz et al., 2005). Stages are indicated in days post-coitum (dpc) from 9.5 dpc onwards. At 8.0–9.0 dpc stages, for better precision, stages are given in somite number (s).

Sections and histological analyses

For histological analyses, embryos were fixed in Carnoy fixative (60% ethanol, 30% chloroform, 3.7% acetic acid), dehydrated and embedded in paraffin. 12 μm serial sections were performed. Sections were stained with cresyl violet/thionine. For cell proliferation studies, embryos were fixed in 4% paraformaldehyde (PFA) in phosphate-buffered saline (PBS), dehydrated and embedded in paraffin. 5 μm sections were performed. For gene expression analyses on sections, embryos were fixed overnight in 4% PFA in PBS, then washed in PBS, embedded in 4% agarose in PBS. 80 μm coronal sections were performed with a vibrating microtome (Leica).

In situ hybridisation

In situ hybridisations (ISH) were performed as described previously (Wilkinson, 1992). The following probes were used: *CRABP1* (Ruberte et al., 1991), *Dlx2* and *Dlx5* (Simeone et al., 1994), *Emx2* (Simeone et al., 1992), *En1* and *En2* (Davis and Joyner, 1988), *Fgf8* (Crossley and Martin, 1995), *Gbx2* (Bouillet et al., 1995), *Hesx1* (Dattani et al., 1998; Thomas and Beddington, 1996), *Hoxb1* (Wilkinson et al., 1989), *Mash1* (Casarosa et al., 1999), *Ngn2* (Ma et al., 1996), *Nkx2.1* (Lazzaro et al., 1991; Shimamura et al., 1995), *Otx2* (Simeone et al., 1992), *Pax6* (Stoykova and Gruss, 1994), *Shh* (Echelard et al., 1993), *Six3* (Oliver et al., 1995), *Sox10* (Kuhlbrodt et al., 1998), *vHnf1/Tcf2* (Cereghini et al., 1992) and *Wnt1* (Wilkinson et al., 1987).

Anti-phospho-histone H3 immunohistochemistry

Whole embryos at 8.5 dpc were fixed overnight in 4% PFA in PBS at 4 °C, washed in PBT (PBS containing 0.1% Tween-20). They were incubated in blocking buffer (BB: PBT supplemented with 5% goat serum) for 1 h at room temperature (RT). Embryos were then incubated for 3 h at RT with the primary antibody (anti-phospho-histone H3 1:100; Upstate, 06-570) in BB. After several washes in PBT, embryos were incubated with goat anti-rabbit biotin-conjugated antibody (Vector) 1:400 in PBT, and stained using the Vectastain Elite ABC Kit (rabbit IgG; Vector) according to the supplier's protocol.

Paraffin sections were rehydrated and digested for 15 min in 20 μg/ml proteinase K solution at RT. They were incubated for 2 h in BB and then for 90 min with the anti-phospho-histone H3 antibody. After several washes in PBT they were incubated for 1 h with the anti-rabbit A488-conjugated (1:1000; Molecular Probes) mixed with DAPI (1:2000; Roche).

TUNEL analyses

At 8.5–9 dpc, whole embryos were processed. At 9.5 dpc and later stages, embryos were embedded in 4% agarose and 50 μm sections were performed with a vibrating microtome. TUNEL staining was made using the Apoptag Apoptosis Detection Kit (Qbiogene) according to the manufacturer's recommendations, with few modifications. Briefly, embryos were digested with 10 μg/ml proteinase K for 5 min at RT and post-fixed in 4% PFA, 0.2% glutaraldehyde in PBT for 20 min. Following the quenching of endogenous peroxidase by 3% H_2O_2 in PBS for 5 min, embryos were incubated in Equilibration Buffer for 30 min at RT, then in Working Strength TdT Enzyme for 1 h at 37 °C. After the stop/wash step, they were incubated overnight at 4 °C in the anti-digoxigenin AP-conjugated antibody 1:2000 in PBT containing 2% sheep serum (Roche). Embryos were then washed and stained for AP activity as described for ISH (Wilkinson, 1992).

Results

Defects in brain and face morphogenesis in Ft/Ft embryos at midgestation

Around midgestation, the morphology of the head was highly perturbed in *Ft/Ft* embryos (Figs. 1B–D) as compared to control siblings (Fig. 1A), with a lot of variability between individuals. The eyes were absent or strongly reduced (arrow in Fig. 1B), the frontonasal process and jaws were hypoplastic, and the brain vesicles were malformed. Folding and closure of the forebrain were delayed. The most severely affected embryos were exencephalic (Fig. 1D). We performed parasagittal (Figs. 1E, F) and coronal (Figs. 1G–M) histological sections through the head of mildly affected 12.5 dpc embryos. In *Ft/Ft* embryos, the general morphology of the brain, and particularly of the forebrain, was severely affected as compared to that of control embryos (Figs. 1E, F). In the telencephalon of control embryos, the telencephalic hemispheres were well separated by the medial pallium, the prospective hippocampus, which formed a medial wall between them. More ventrally, in the subpallium, the medial and lateral ganglionic eminences were clearly visible (Fig. 1G). In *Ft/Ft* embryos, the telencephalic vesicles were not so clearly subdivided, and the medial pallium was reduced or absent (Figs. 1F, H). This may be related to the delay in dorsal forebrain folding and closure, apparent at earlier stages (see below and data not shown). In the subpallium, only one ganglionic eminence could usually be observed (Fig. 1H). More caudally, the diencephalon and midbrain were also malformed (Fig. 1F). Eye rudiments could be detected at internal positions. The retina was small and its shape was irregular, while the lens was often hardly detectable (Figs. 1J, K). The anterior lobe of the pituitary, normally located adjacent to the ventral diencephalon (Fig. 1L), was reduced or absent in *Ft/Ft* embryos (Fig. 1M and data not shown). In the facial region, the frontonasal process was hypoplastic (Fig. 1F), the nasal cavity was widely open to the outside (Fig. 1H) and the mouth was malformed (Figs. 1E–H). Therefore, morphogenesis of both the brain and the face are severely affected in *Ft/Ft* embryos.

Anteroposterior patterning of the brain

In order to determine the origin of the defects seen at midgestation, we analysed brain patterning at earlier stages. At early somite stages, the morphology of the brain was already affected in *Ft/Ft* embryos: the anterior neural plate was abnormally folded (Fig. 2 and data not shown). To better understand brain abnormalities, we performed in situ hybridisations (ISH) for genes specifically expressed in distinct domains of the neural plate.

The expression patterns of several genes, such as *Fgf8*, *Six3*, *Hesx1* and *Pax6*, subdivide the forebrain into distinct AP domains at the onset of somitogenesis. The expression of *Hesx1* (Thomas and Beddington, 1996) (Fig. 2B) and *Six3* (Oliver et al., 1995) (Fig. 2D) is activated during gastrulation in the anterior neural plate, and persists in this domain during early somite stages. *Fgf8* is expressed in the anterior neural ridge (ANR) (Shimamura and Rubenstein, 1997) (Fig. 2F). *Pax6* is expressed from early somite stages onwards in the whole forebrain region, up to the forebrain–midbrain boundary (Stoykova and Gruss, 1994) (Figs. 2H, J). In *Ft/Ft* embryos at early somite stages, the expression domains of *Hesx1*, *Six3*, *Fgf8* and *Pax6* in the forebrain were expanded posteriorly (Figs. 2C, E, G, I), as compared to control embryos (Figs. 2B, D, F, H). The caudal expansion of *Six3* was detected as early as the 2 s stage (data not shown). In contrast, the expression domain of *Otx2*, a marker of both the prospective forebrain and midbrain (Simeone et al., 1993) (Fig. 2L) was not expanded (Fig. 2M). In double ISH experiments, the *Pax6*-negative, *Otx2*-positive domain corresponding to the future midbrain was strongly reduced in *Ft/Ft* embryos (Figs. 2J, K). In conclusion, the whole forebrain is expanded in *Ft/Ft* embryos, whereas the midbrain appears reduced.

We further analysed the subdivision of the neural plate in the midbrain–hindbrain region. *Wnt1*, *En1* and *En2* show a dynamic expression pattern in this region at 8.0–9.0 dpc (Bally-Cuif and Wassef, 1995). All three genes are initially expressed in a broad domain centered on the midbrain–hindbrain boundary (MHB), at a high level at the MHB and in decreasing gradients anterior and posterior to this boundary (Figs. 2D, N, P). The expression of *En1 and En2* extends more caudally than that of *Wnt1*. Later, at 9.5 dpc, *Wnt1* and *En1* expression domains restrict to a ring at the MHB (data not shown). *Fgf8* expression is also dynamic in this region. It first covers the metencephalic vesicle and then restricts to a ring of cells just caudal to the *Wnt1* ring (Bally-Cuif and Wassef, 1995) (Figs. 2F, T). In *Ft/Ft* embryos at early somite stages, the *Wnt1* and *En1* expression domains were shorter along the AP axis (Figs. 2E, O). Moreover, the posterior-to-anterior decreasing gradient in the midbrain, characteristic of these genes, was absent. Instead, the sharp anterior boundary of *Wnt1* expression abutted the caudal boundary of *Pax6* expression (Fig. 2O). Caudally to the MHB, *Fgf8* expression in the metencephalon was similar in *Ft/Ft* and in control embryos (Figs. 2F, G). More caudal hindbrain markers, such as *Hoxb1* expression in r4 and *Vhnf1* expression caudally to the r4/r5 boundary, were not significantly modified in *Ft/Ft* embryos (Figs. 2D, E, L and M).

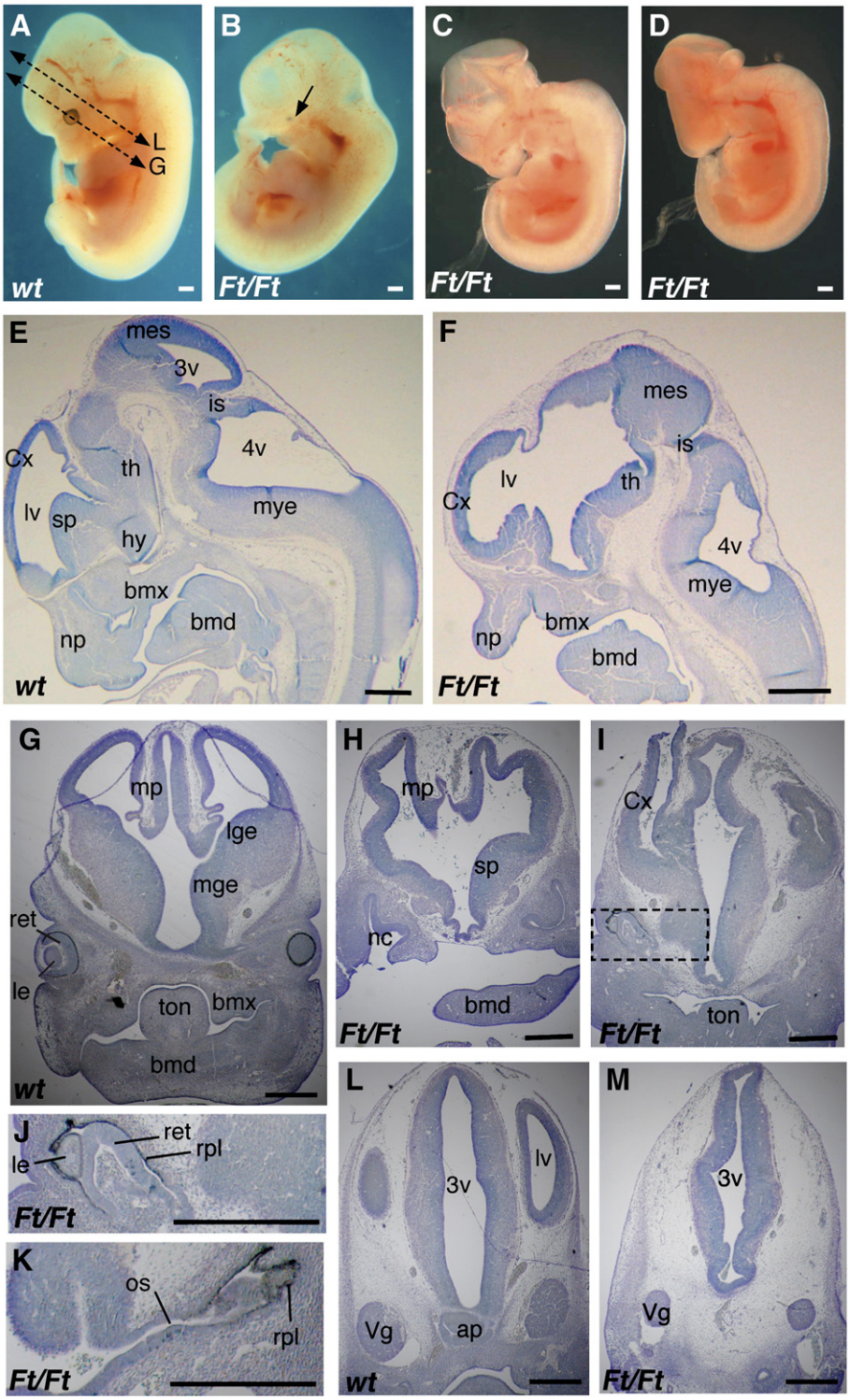

Fig. 1. Morphological and histological analysis of the brain and head of *Ft* embryos at 12.5 dpc. (A, D) Morphology of a wild type (A) and three homozygous *Ft* (B–D) embryos. The dotted double arrows in panel A indicate the planes of coronal sections in panels G and L. The arrow in panel B indicates the reduced eye. (E, F) Parasagittal sections of wild type (E) and *Ft/Ft* (F) embryos stained with cresyl–thionine. (G–M) Coronal sections of wild type (G, L) and *Ft/Ft* (H–K, M) embryos stained with cresyl–thionine. Panel J is a higher magnification of the region squared in panel I. Ap: anterior lobe of the pituitary gland; bmd: mandibular process of BA1; bmx: maxillary process of BA1; Cx: cerebral cortex; hy: hypothalamus; is: isthmus; le: lens; lge: lateral ganglionic eminence; lv: lateral ventricle; mes: mesencephalon; mge: medial ganglionic eminence; mp: medial pallium; mye: myelencephalon; nc: nasal cavity; np: nasofrontal process; os: optic stalk; rpl: retinal pigmented layer; sp: subpallium; ret: retina; th: thalamus; ton: tongue; 3v: third ventricle; 4v: fourth ventricle, Vg: trigeminal ganglion. Scale bars are 500 μm.

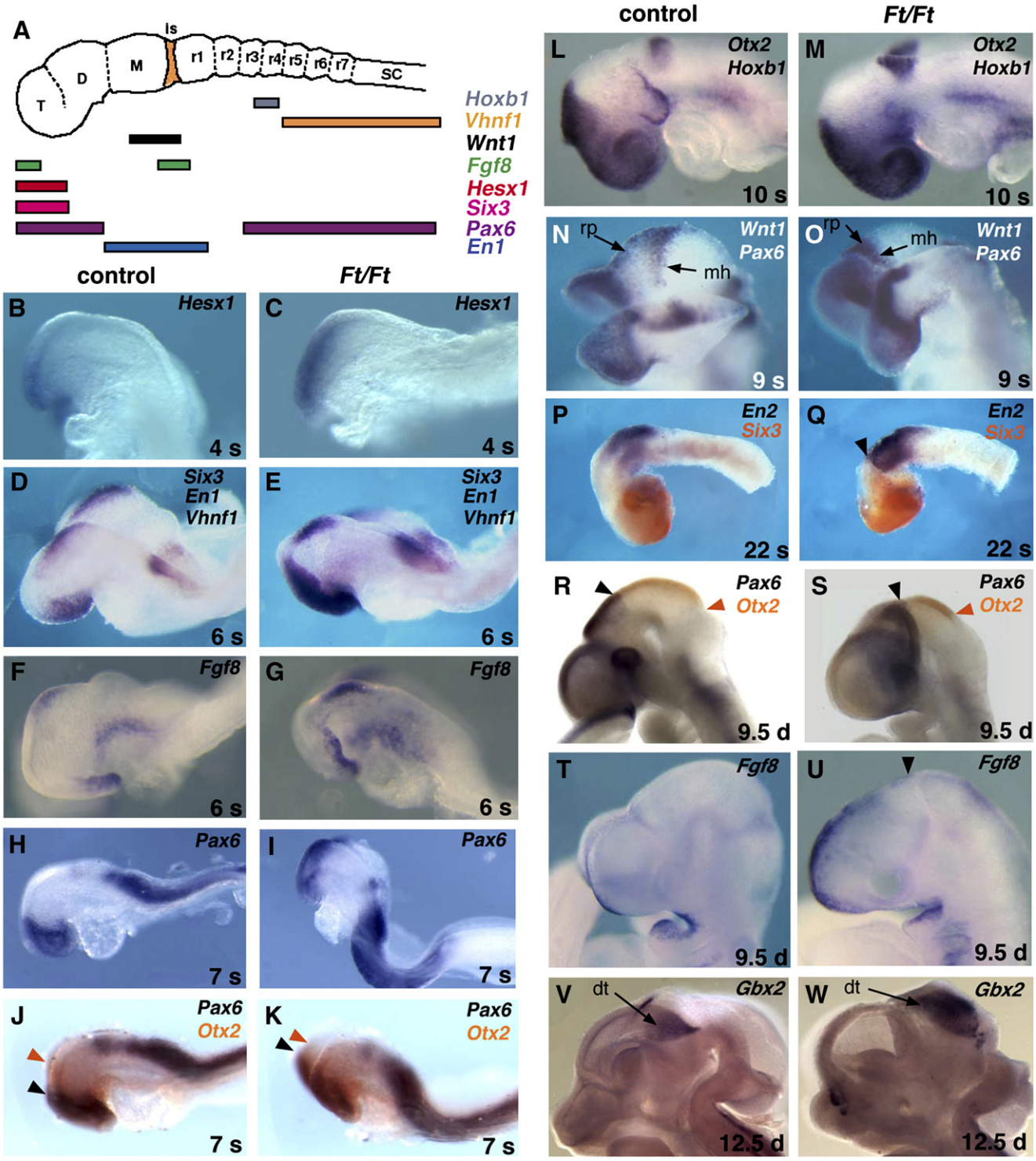

Fig. 2. ISH analysis of AP brain patterning in *Ft* embryos. (A) Schematic representation of gene expression patterns in the 8.5 dpc mouse brain. (B–W) ISH analysis of control (B, D, F, H, J, L, N, P, R, T, V) and *Ft/Ft* (C, E, G, I, K, M, O, Q, S, U, W) embryos using probes for the *Hesx1* (B, C), *Six3* (D, E, P, Q), *Fgf8* (F, G, T, U), *En1* (D, E), *Vhnf1* (D, E), *Pax6* (H–K, N, O, R, S), *Wnt1* (N, O), *Hoxb1* (L, M), *En2* (P, Q) *Otx2* (J–M, R, S) and *Gbx2* (V, W) genes. All embryos are lateral views oriented with anterior to the left. Panels V and W are half heads obtained by sagittal section and viewed from the ventricular side. In double and triple ISH experiments shown in panels D, E, L, M, N and O, all probes are stained in purple. In double ISH shown in panels J, K, P–S, *En2* and *Pax6* are purple and *Six3* and *Otx2* are red. Black arrowheads in panels Q, S and U indicate the morphological discontinuity at the forebrain–midbrain boundary in *Ft/Ft* embryos. Black and orange arrowheads in panels J, K, R and S indicate the caudal limit of *Pax6* and *Otx2* expression domains, respectively. The embryonic stages are indicated at the bottom right of the pictures. d: dpc; dt: dorsal thalamus; mh: midbrain–hindbrain domain; rp: roof plate.

At 9.0–9.5 dpc, the morphology of the brain was disrupted in *Ft/Ft* embryos, although the severity of the defects was variable (Figs. 2 and 3). Common features were: smaller forebrain and midbrain, defects in medial septation of the telencephalic vesicles, and abnormal shape of the optic vesicles. Accordingly, the larger expression domains of *Six3* and *Pax6* seen at earlier stages were not detectable anymore (Figs. 2P–S). In contrast, the expression domain of *Fgf8* in the forebrain was still expanded (Figs. 2T, U). In *Ft/Ft* embryos, this domain now encompassed not only the derivatives of the ANR as in control embryos (Fig. 2T) but also the dorsal midline of the prospective telencephalon (Fig. 2U). The reduction of the midbrain was confirmed at this stage by double ISH with *Pax6* and *Otx2*: the *Pax6*-negative, *Otx2*-positive domain, corresponding to the midbrain, was shortened along the AP axis by about one half (Figs. 2R, S). *En2* was expressed at an abnormally high level in the whole midbrain and in the anterior hindbrain, with a sharp anterior limit at the forebrain–midbrain boundary (Fig. 2Q), contrasting with the anteriorly decreasing gradient observed in control embryos (Fig. 2P). This anterior limit coincided with a prominent morphological boundary (black arrowheads in Figs. 2Q, S, U) that contrasted with the smooth forebrain–midbrain boundary seen in control embryos (Figs. 2P, R, T).

To further investigate patterning of the caudal part of the forebrain, we analysed the expression of *Gbx2*, a gene expressed in the dorsal thalamus (caudal diencephalon), just caudal to the ZLI (Bulfone et al., 1993b). *Gbx2* was expressed in the caudal diencephalon of both control (Fig. 2V) and *Ft/Ft* (Fig. 2W) embryos at 12.5 dpc. The *Gbx2* positive domain appeared expanded caudally in homozygous embryos, with may reflect a reduction or absence of more caudal regions such as the pretectum and anterior midbrain.

In conclusion, several aspects of brain AP patterning are affected in homozygous *Ft* embryos. (i) The forebrain is expanded at 8.0–8.5 dpc, but this expansion does not persist and only *Fgf8* expression in the derivatives of the ANR remains expanded at later stages. (ii) The midbrain is reduced in size, and genes such as *Wnt1* and *En1*/2 show a homogenous

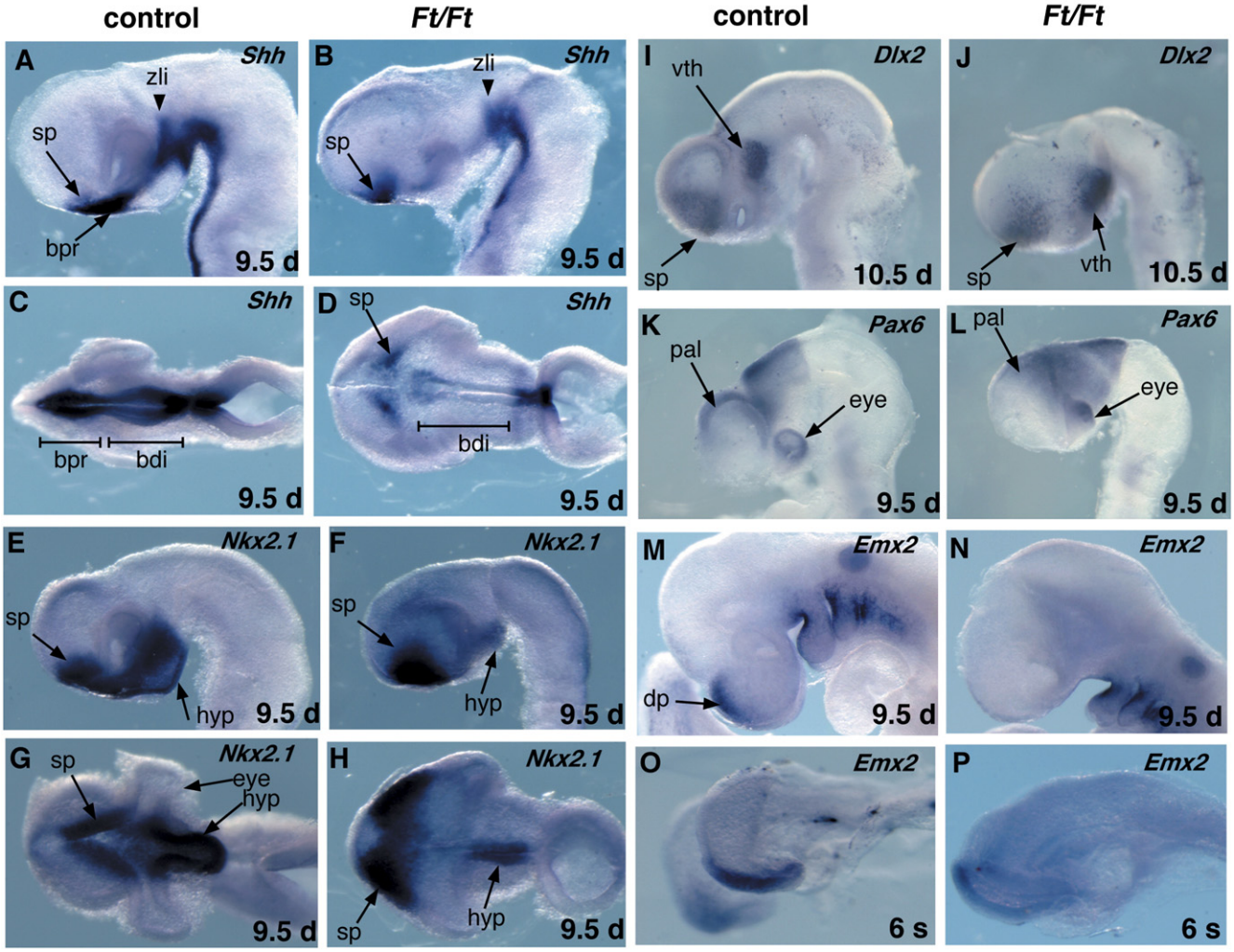

Fig. 3. ISH analysis of DV brain patterning in *Ft* embryos. Control (A, C, E, G, I, K, M, O) and *Ft/Ft* (B, D, F, H, J, L, N, P) embryos were stained by ISH with probes for the *Shh* (A–D), *Nkx2.1* (E–H), *Dlx2* (I, J), *Pax6* (K, L) and *Emx2* (M–P) genes. All embryos are oriented with anterior to the left. Panels A, B, E, F, I–L are lateral views of dissected brains; panels C, D, G and H are ventral views of dissected brains; panels M–P are lateral views of whole embryos. The embryonic stages are indicated at the bottom right of the pictures. bdi: diencephalon; bpr: basal prosencephalon; d: dpc; dp: dorsal pallium; hyp: hypothalamus; pal: pallium; sp: subpallium; vth: ventral thalamus; zli: *zona limitans intrathalamica*.

expression in the whole midbrain domain, which contrasts with their usual posterior-to-anterior decreasing gradient. (iii) At the junction between these two domains, the forebrain–midbrain boundary forms an abnormally prominent morphological discontinuity.

Dorsoventral patterning of the brain

Having analysed in detail the AP patterning of the brain in *Ft/Ft* embryos, we wished to investigate its DV patterning. The abnormal morphogenesis of the telencephalon observed at 12.5 dpc suggests defects in DV patterning of the forebrain. Such defects would be consistent with previous observations of altered DV patterning of the spinal cord and loss of the floor plate in *Ft/Ft* embryos after 9.0 dpc (Götz et al., 2005).

In order to investigate DV patterning of the brain, we first analysed the expression of the ventral marker *Shh*. In control embryos at 9.5 dpc, *Shh* is expressed in a longitudinal domain in the ventral forebrain (Figs. 3A, C) with a dorsal extension within the diencephalon that prefigures the ZLI (arrowhead in Fig. 3A). In *Ft/Ft* embryos, the expression of *Shh* in the brain was fainter and fuzzier (Figs. 3B, D), as has already been described in more caudal regions of the CNS (Götz et al., 2005). The telencephalic (subpallial) expression domain of *Shh* was maintained in *Ft/Ft* embryos (arrow in Fig. 3D). In contrast, its expression in the basal diencephalon anterior to the ZLI was strongly reduced or absent (Figs. 3B, D).

We then analysed the expression of the ventral forebrain marker *Nkx2.1*, a target of Shh signalling. *Nkx2.1* is expressed at 8.5 dpc in the ventromedial region of the forebrain (Shimamura et al., 1995). Later, it is expressed in the basal plate of the prosencephalon – the prospective hypothalamus – and also, from 9.5 dpc onwards, in the ventral telencephalon (subpallium). In *Ft/Ft* embryos, the *Nkx2.1* expression domain in the prospective hypothalamus was strongly reduced (Figs. 3F, H) as compared to that observed in control embryos (Figs. 3E, G). In contrast, its telencephalic expression was maintained and expanded laterally in homozygous *Ft* embryos (Figs. 3F, H).

Dlx2 is normally expressed in the subpallium, in the prospective ganglionic eminences, and in the ventral thalamus—a diencephalic domain located just anterior to the ZLI (Bulfone et al., 1993a). In *Ft/Ft* embryos, *Dlx2* expression was not strongly altered (Figs. 3I, J). However, its diencephalic expression extended more ventrally (Fig. 3J) than in control embryos (Fig. 3I), consistent with the reduction of the hypothalamus.

In order to determine whether the dorsal forebrain was affected, we analysed *Pax6* expression at 9.5 dpc (Figs. 3A, B). At this stage, *Pax6* is expressed in the dorsal telencephalon – the pallium – and in the dorsal diencephalon (Marin and Rubenstein, 2002; Stoykova and Gruss, 1994). While in the telencephalon, the *Pax6* expression domain was restricted to the dorsal part in both control and *Ft/Ft* embryos, in the diencephalon it expanded more ventrally in *Ft/Ft* embryos (Figs. 3K, L). Similarly to *Dlx2*, the ventral shift of *Pax6* in the diencephalon may be a consequence of the reduction of the hypothalamus.

Emx2 is expressed in the latero-caudal part of the forebrain starting at the 3 s stage (Shimamura et al., 1995) (Fig. 3O). At 9.5 dpc, *Emx2* expression restricts to the dorsal telencephalon (Shimamura et al., 1995) (Fig. 3M). In *Ft/Ft* embryos at 9.5 dpc, *Emx2* expression was severely reduced or absent (Fig. 3N). This phenotype was already observed at early somite stages (Fig. 3P).

Patterning defects in the brain of *Ft* mutants could result in changes in neuronal specification. In the telencephalon, inhibitory GABAergic neurons are born in the subpallium, while excitatory glutamatergic neurons are born in the pallium (Marin and Rubenstein, 2002). These domains of distinct neuronal specificity are prefigured by the complementary expression of the proneural genes, *Mash1* in the subpallium (Figs. 4A, C) and *Neurogenin2* (*Ngn2*) in the pallium (Figs.

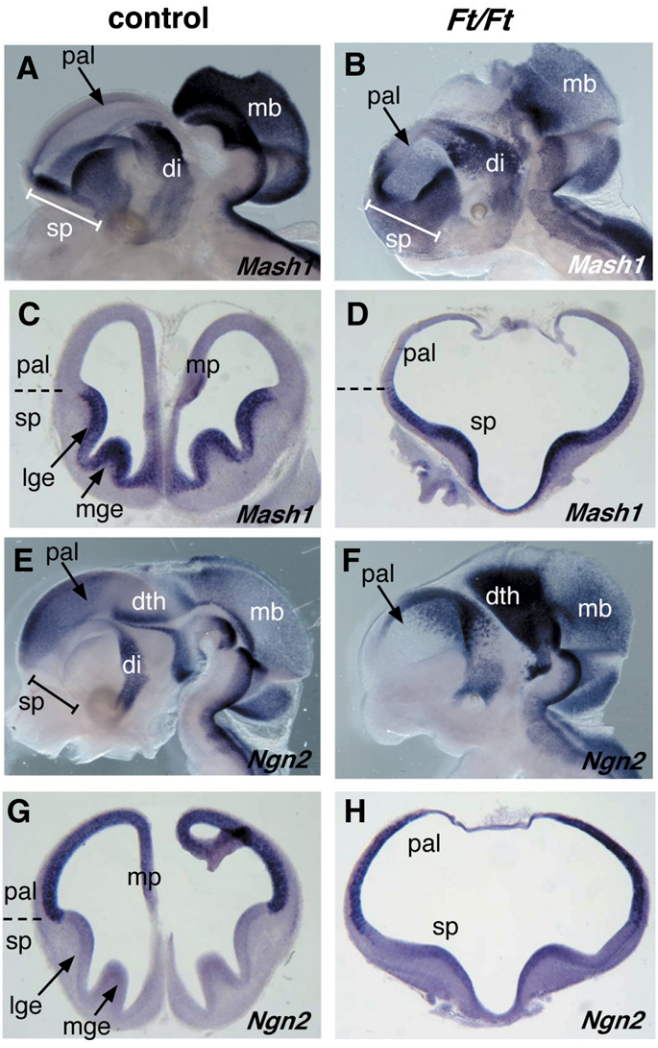

Fig. 4. ISH analysis of neurogenesis in the telencephalon of *Ft* embryos. Control (A, C, E, G) and *Ft/Ft* (B, D, F, H) 12.5 dpc embryos were labelled with probes for the *Mash1* (A–D) and *Ngn2* (E–H) genes. Panels A, B, E and F are half heads obtained by sagittal section and viewed from the ventricular side (panels B and F are half heads of the same *Ft/Ft* embryo). Panels C, D, G and H are 80 μm coronal sections in the telencephalic region. di: diencephalon; lge: lateral ganglionic eminence; mge: medial ganglionic eminence; mb: midbrain; mp: medial pallium; pal: pallium; sp: subpallium.

4E, G) (Casarosa et al., 1999; Ma et al., 1996). These two complementary expression domains present a sharp limit at the pallial/subpallial boundary (Figs. 4C, G). We tested whether the patterning defects in the telencephalon of *Ft/Ft* embryos had any consequence on the expression patterns of *Ngn2* and *Mash1*. In 12.5 dpc *Ft/Ft* embryos, *Mash1* expression in the telencephalon was present and expanded dorsally in the anterior part of the pallium (Fig. 4B). Conversely, *Ngn2* expression was maintained in the posterior pallium but was reduced in the anterior pallium (Fig. 4F). The two expression domains were still complementary, but their common limit at the pallial–subpallial boundary was fuzzier (Figs. 4D, H) than in control embryos (Figs. 4C, G). Therefore, while the subdivision of the telencephalon into pallial and subpallial domains of neurogenesis is maintained in homozygous *Ft* mutants, the respective size of these two domains is modified.

Mash1 and *Ngn1* expression in the diencephalon appeared also modified in homozygous embryos. In particular, *Ngn2* expression in the dorsal thalamus is expanded and is much stronger than in control embryos, consistent with an expansion of *Gbx2* expression in this domain (see above).

In conclusion, DV regionalisation of the forebrain is abnormal in *Ft/Ft* embryos. In particular, two regions are severely reduced or absent: the hypothalamus (which expresses *Nkx2.1*) and the medial pallium (which expresses *Emx2*). The medial pallium corresponds to the dorsomedial part of the telencephalic vesicles, which themselves derive from the alar plate of the forebrain (Marin and Rubenstein, 2002). The hypothalamus, in contrast, derives from the basal plate of the forebrain. Therefore, we conclude from these observations that both the most ventral and the most dorsal parts of the forebrain are severely reduced in *Ft/Ft* embryos.

Cell proliferation and cell survival in the brain of Ft mutant embryos

Our analysis of gene expression patterns showed that several regions of the brain were reduced or absent in homozygous *Ft* embryos. This reduction of the size of brain domains could reflect changes in the fate of neuroepithelial cells. Alternatively, it could result from changes in the rate of proliferation of these cells or from increased apoptosis. In order to test these hypotheses, we first investigated cell proliferation by staining embryos for phosphorylated histone H3, a marker of mitotic cells. We did not see any significant difference in the proportion of neuroepithelial cells stained by H3P in different brain regions between control and *Ft/Ft* embryos at 8.5 dpc (8 to 15 s) (Figs. 5A, B), 9 dpc (20 to 25 s) (data not shown) and 9.5 dpc (30–35 s) (Figs. 5C, D). Then, to label apoptotic cells, we performed TUNEL staining on embryos from 8.0 dpc to 10.5 dpc. To our surprise, homozygous *Ft* embryos showed extensive cell death in the anterior forebrain (Figs. 5E–J). No significant difference in the rate of cell death was found between control and *Ft/Ft* embryos at the 4 s stage (data not shown). The increased cell death was detected as soon as the 7 s stage in the ANR of *Ft/Ft* embryos (Figs. 5E, F), and was even more dramatic at the 15 s stage (Figs. 5G, H). At E9.5, both the anterior telencephalon and

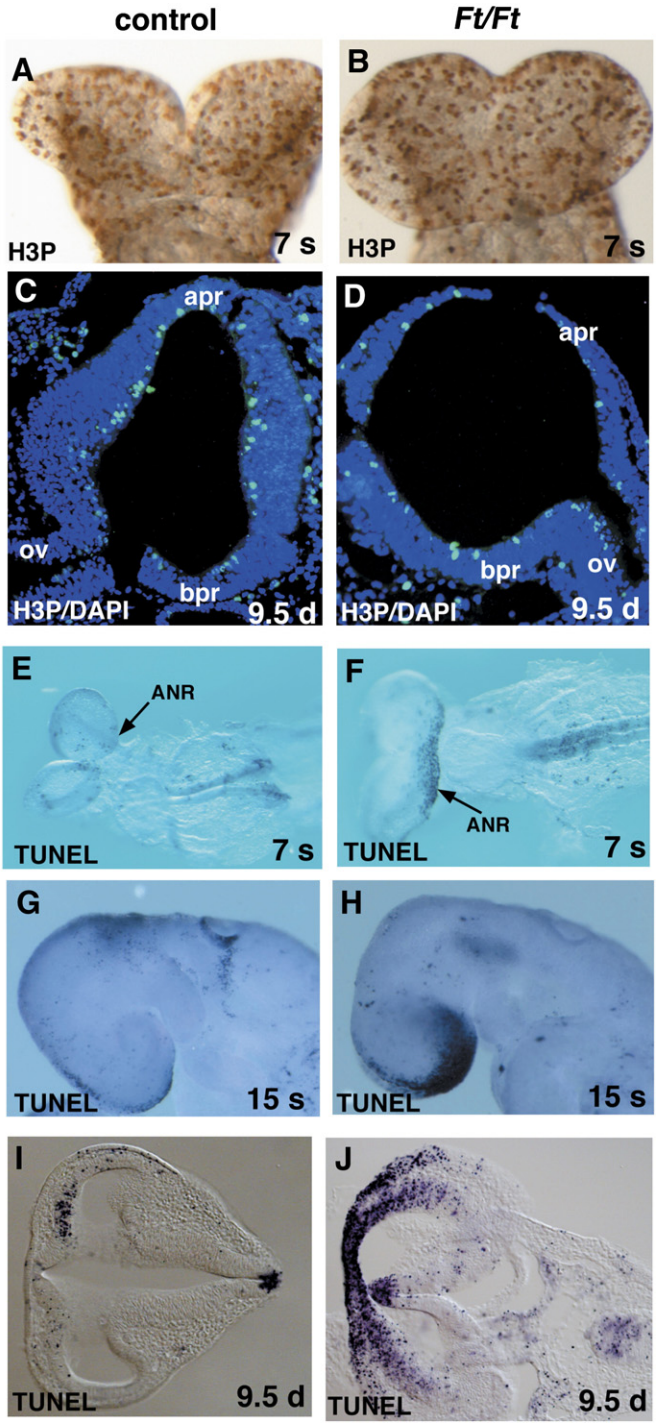

Fig. 5. Analysis of cell proliferation and cell death in *Ft* mutant embryos. (A, B) Control (A) and *Ft/Ft* (B) embryos at the 7 s stage stained by immunohistochemistry with an antibody for phosphorylated Histone H3 (H3P). (C, D) Control (C) and *Ft/Ft* (D) embryos at 9.5 dpc stained for H3P (green) and DAPI (blue). (E–J) TUNEL experiments on control (E, G, I) and *Ft/Ft* (F, H, J) embryos at the 7 s (E, F), 15 s (G, H) and 9.5 dpc (I, J) stages. Panels A and B show frontal views of the head region of whole embryos. Panels C and D show coronal sections through the forebrain, with anterior up. Panels E and F show ventral views of embryos oriented anterior to the left. Panels G and H show lateral views of the head region of embryos oriented with anterior to the left. Panels I and J are 50 μm coronal sections through the head, with anterior to the left. ANR: anterior neural ridge; apr: alar plate of the prosencephalon; bpr: basal plate of the prosencephalon; d: dpc; ov: otic vesicle.

the anterior ectoderm showed a high level of cell death (Figs. 5I, J). These results, combined with the gene expression data presented above, show that, in *Ft/Ft* embryos: (i) the expansion of the forebrain at 8.5 dpc, as well as the reduction of the midbrain and of the hypothalamus, do not result from variations in cell proliferation or cell survival, but rather from cell fate changes and (ii) extensive cell death in the ANR and its derivatives is a likely cause of forebrain reduction at 9.5 dpc and later stages.

Neural crest and branchial arch formation

Head morphogenesis is severely affected in *Ft/Ft* embryos around midgestation. Since many craniofacial structures derive from, or depend on, the neural crest for their morphogenesis, we investigated neural crest formation and migration in *Ft* embryos. To this end, we analysed the expression of two genes expressed in neural crest cells (ncc), *Sox10* and *CRABP1*. *Sox10* expression is initiated in ncc as they dissociate from the neural tube, and is maintained during ncc migration (Kuhlbrodt et al., 1998). *CRABP1* is expressed in migratory ncc and is maintained in the mesenchyme of the branchial arches – but faintly in BA1 – and in the frontonasal mass (Maden et al., 1992; Ruberte et al., 1991). In control embryos, *Sox10* expression in migrating ncc was detected at the 6 s stage in the prospective head region and then, at the 9 s stage, in more posterior regions (Figs. 6A, C, and data not shown). *Sox10* ISH showed a delay of ncc migration in the head of *Ft/Ft* embryos as compared to controls, while ncc migration in the trunk appeared normal (Figs. 6A–D). *CRABP1* staining at later stages showed that ncc eventually reached their final destination in the frontonasal mass and branchial arches both in control (Figs. 6E, G) and in *Ft/Ft* (Figs. 6F, H) embryos. In order to confirm the migration of ncc in the branchial arches, we analysed the expression of *Dlx2* and *Dlx5*. Both genes are expressed in the post-migratory ncc in the branchial arches (Qiu et al., 1997), and their expression subdivides the branchial arches along the proximodistal axis. *Dlx2* is expressed along all the proximodistal axis (Fig. 6I), whereas *Dlx5* is expressed in the distal part only (Fig. 6K) (Qiu et al., 1997). In *Ft/Ft* embryos at 9.5–10.5 dpc, the branchial arches were much smaller than in control embryos, but *Dlx2* and *Dlx5* were expressed with normal patterns and intensity (Figs. 6J, L and data not shown).

In conclusion, in *Ft/Ft* embryos, ncc migration in the head shows a normal pattern, but is delayed compared to control embryos. This defect correlates with the reduction in size of the branchial arches at 9.5–10.5 dpc, and is a likely cause of the hypoplasia of the nasal process and branchial arches observed at 12.5 dpc.

Discussion

In this paper we present an analysis of early brain and craniofacial defects in *Ft/Ft* embryos. The *Ft* line carries a 1.6 Mb deletion, eliminating 6 genes: three genes coding for transcription factors of the Iroquois family, *Irx3*, *Irx5* and *Irx6*,

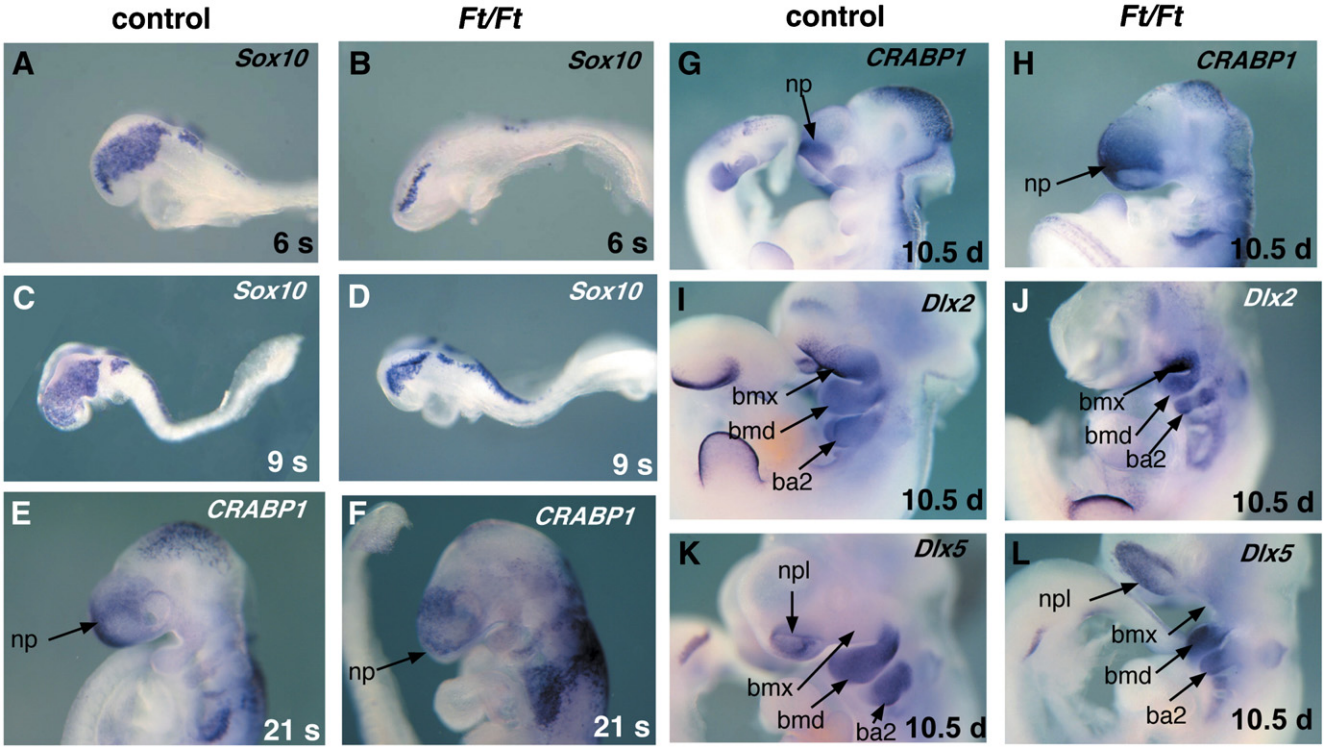

Fig. 6. Analysis of neural crest migration and branchial arch formation in *Ft* embryos. (A–D) 6 s (A, B) or 9 s (C, D) control (A, C) or *Ft/Ft* (B, D) embryos stained with a *Sox10* probe. (E–H) 21 s (E, F) or 10.5 dpc (G, H) control (E, G) and *Ft/Ft* (F, H) embryos stained with a *CRABP1* probe. (I, J) 10.5 dpc control (I) and *Ft/Ft* (J) embryos stained with a *Dlx2* probe. (K, L) 10.5 dpc control (K) or *Ft/Ft* (L) embryos stained with a *Dlx5* probe. All embryos are oriented with anterior to the left. ba2: 2nd branchial arch; bmd: mandibular part of BA1; bmx: maxillary part of BA1; d: dpc; np: nasal process; npl: nasal placode.

and three novel genes of unknown function: *Fts*, *Ftm* and *Fto* (Peters et al., 2002). Although the phenotype of *Ft/Ft* embryos at midgestation is complex and variable, it can be traced back to several striking patterning defects observed as soon as the beginning of somitogenesis. This, together with the previously published expression patterns of *Irx* genes, allows us to propose that some of the phenotypes are due to the absence of the *IrxB* complex.

Both AP and DV patterning of the brain are affected in Ft/Ft embryos

Defects in AP regionalisation of the brain are apparent as soon as 8.25 dpc in *Ft/Ft* embryos. At this stage, the expression domains of *Six3*, *Hesx1*, *Fgf8* and *Pax6* in the anterior neural plate are expanded. At the same stage, the prospective midbrain is strongly reduced along the AP axis, as seen by double ISH with *Wnt1* and *Pax6*. Changes in the rate of cell proliferation or cell death are not responsible for these phenotypes. Therefore, they are most probably due to changes in cell identity. Our observations provide two possible, non exclusive explanations for the expansion of forebrain fates. First, the ANR is expanded. Since this organising centre is known to be a source of signals involved in patterning the forebrain (Shimamura et al., 1997; Wilson and Houart, 2004), its expansion could lead to a caudal expansion of the forebrain. Second, the reduction of the midbrain is consistent with a mis-specification of the anterior midbrain into forebrain fate, and this could lead to a more caudal positioning of the forebrain–midbrain boundary.

DV regionalisation of the forebrain is also affected in *Ft/Ft* embryos. Surprisingly, two regions located at opposite DV positions are severely reduced: the hypothalamus, a ventral forebrain-derived structure, and the medial pallium, which forms in most dorsal region of the forebrain (Marin and Rubenstein, 2002). The reduction of the hypothalamus could be due to a defect in the Shh pathway: mutants in this pathway show a loss of ventral brain structures (Chiang et al., 1996, Park et al., 2000), and Shh can induce *Nkx2.1* expression and hypothalamus formation in anterior neural plate explants (Ericson et al., 1995; Shimamura and Rubenstein, 1997). In contrast, in the dorsal forebrain, some aspects of the phenotype of *Ft/Ft* embryos are similar to that described for mice mutant for *Gli3*, which codes for a repressor of the Shh pathway (Kuschel et al., 2003; Theil et al., 1999; Tole et al., 2000). Common features include defects in septation of the telencephalic vesicles and absence of the hippocampus – a derivative of the medial pallium – absence of telencephalic *Emx2* expression, and expansion of *Fgf8* expression in the ANR. However, both phenotypes also show distinct features: In *Gli3* homozygous embryos, cell death in the anterior brain is reduced, whereas it is enhanced in *Ft/Ft* embryos. *Ft* mice have been proposed to be affected in the Shh pathway, based on their phenotype in the spinal cord (Götz et al., 2005). Here we describe brain phenotypes that support this proposal, but the exact molecular nature of the defect is not clear.

Some of the patterning defects observed in the telencephalon could also result from the expansion of the *Fgf8* expression domain in the ANR. Three signalling centers, the ANR and the dorsal and ventral midlines, interact to pattern the telencephalon (Shimogori et al., 2004; Storm et al., 2006). Fgf8 signalling from the ANR represses the expression of *Wnt* genes in the dorsal midline and of *Emx2* in the dorsocaudal telencephalon (Storm et al., 2006). Moreover, an excess of Fgf8 signalling leads to increased cell death in the anterior telencephalon (Storm et al., 2003). Therefore, both the reduction of *Emx2* expression and the extended cell death observed in the telencephalon of *Ft/Ft* embryos could well be a consequence of the expansion of the *Fgf8* expression domain in the ANR. The precise mechanism by which this expansion occurs remains to be determined.

Head morphogenesis is abnormal in Ft mutants

Head morphogenesis is abnormal in *Ft/Ft* embryos. Although the severity of the phenotype is variable, common features can be identified. The first one is the incomplete septation of the telencephalic vesicles, which leads to exencephaly in the most severe cases. This phenotype can be traced back to the abnormal folding of the anterior neural plate observed as soon as 8.5 dpc, and to the delay in anterior neural tube closure. Interestingly, mutants affected in medial pallium formation, such as the *Gli3* mutants (Theil et al., 1999) or double mutants for *Emx1* and *Emx2* (Shinozaki et al., 2004), show defects in septation of the telencephalic vesicles similar to that of *Ft* mutants. This suggests that, in *Ft/Ft* embryos, the loss of the medial pallium could be a cause of the abnormal anterior neurulation.

Another aspect of head morphogenesis in *Ft/Ft* embryos is the reduction of the nasal process and of the branchial arches, which together form the architecture of the face. Since *Ft* homozygous embryos die around midgestation, it was not possible to analyse precisely facial architecture in these mutants. However, at early stages, we observed anomalies in two embryonic structures that participate in craniofacial morphogenesis, the neural crest and the branchial arches. First, neural crest migration toward the nasal process, the periotic region, and branchial arches 1 and 2, is delayed in *Ft/Ft* embryos as compared to controls. Second, although the branchial arches appear normally patterned, they are smaller in *Ft/Ft* embryos than in control embryos. Facial morphogenesis is a highly complex process that involves the interaction of many distinct cell types (for review, Depew et al., 2002). While the observed delay in neural crest migration is a possible cause of facial hypoplasia, further analyses will be required to confirm this hypothesis.

The loss of the IrxB cluster is a likely cause of the AP patterning defects

The *Ft* deletion eliminates six genes, among which the whole *IrxB* complex. The expression patterns of two genes of this complex, *Irx3* and *Irx5*, suggest that their absence could be responsible for some of the defects observed in *Ft/Ft* embryos. Between 8 and 9 dpc, *Irx3* and *Irx5* show very similar

expression patterns, being restricted to the midbrain and hindbrain (Bosse et al., 1997; Houweling et al., 2001). The expression of *Irx3* is detected earlier, as soon as 7.5 dpc, in the neural plate (Bellefroid et al., 1998; Bosse et al., 1997; Houweling et al., 2001). After 9 dpc, in addition to these sites, *Irx3* is also expressed in the pretectum and dorsal thalamus, in the cephalic mesoderm around the eye and in the ectoderm of the first branchial arch. *Irx6* is not expressed before 10.5 dpc, so its elimination cannot be responsible for the early phenotypes described in this paper.

Because the anterior limit of *Irx3* and *Irx5* expression before 9 dpc lies at the forebrain–midbrain boundary, we propose that the loss of both genes in the *Ft* mutant line is responsible for the reduction in size of the midbrain, and, as a consequence, for the caudal expansion of the forebrain. Interestingly, ectopic expression of *Irx3* by electroporation in the chicken neural tube has shown that this gene was involved in specifying caudal versus rostral diencephalic fate, and in positioning the boundary between these two domains, the future ZLI (Kobayashi et al., 2002). However, in *Ft/Ft* embryos, both rostral and caudal diencephalon are specified, as shown by ISH for *Dlx2* (Fig. 3J) and *Gbx2* (Fig. 2W). This may be due to a functional compensation by members of the *IrxA* gene cluster.

It is unlikely that the absence of genes of the *IrxB* complex causes the defects in the telencephalon and hypothalamus observed in *Ft/Ft* embryos, since *Irx* genes are not expressed anterior to the ZLI. Therefore, one of the other genes eliminated by the *Ft* deletion, *Fts*, *Ftm* and *Fto* must have a function in DV patterning of the forebrain. All three genes are expressed widely during embryogenesis (Lesche et al., 1997; Peters et al., 1999; Rüther, unpublished data). The contribution of each of the six candidate genes to the *Ft* phenotype will require the generation of knock-out mice for the individual genes. A mutant for one of these genes, *Irx5*, has already been described in the literature. *Irx5* homozygous mutant mice are viable and fertile, and no brain phenotype has been characterised so far (Costantini et al., 2005). However, given the similarity in the expression patterns of *Irx3* and *Irx5* during somitogenesis, a functional compensation may exist, and the full understanding of their function may require the obtainment of double mutants.

Acknowledgments

We thank François Giudicelli and Virginie Lecaudey for critical reading of the manuscript. This work was supported by grants from Centre National de la Recherche Scientifique, Université Pierre et Marie Curie, Institut National pour la Santé et la Recherche Médicale, and Association pour la Recherche sur le Cancer.

References

Ang, S.-L., Behringer, R.R., 2002. Anterior–posterior patterning of the mouse body axis at gastrulation. In: Rossant, J., Tam, P.P. (Eds.), Mouse Development: Patterning, Morphogenesis, and Organogenesis. Academic Press, San Diego, pp. 37–49.

Bally-Cuif, L., Wassef, M., 1995. Determination events in the nervous system of the vertebrate embryo. Curr. Opin. Genet. Dev. 5, 450–458.

Bellefroid, E.J., Kobbe, A., Gruss, P., Pieler, T., Gurdon, J.B., Papalopulu, N., 1998. *Xiro3* encodes a *Xenopus* homolog of the *Drosophila Iroquois* genes and functions in neural specification. EMBO J. 17, 191–203.

Bosse, A., Zulch, A., Becker, M.B., Torres, M., Gomez-Skarmeta, J.L., Modolell, J., Gruss, P., 1997. Identification of the vertebrate *Iroquois* homeobox gene family with overlapping expression during early development of the nervous system. Mech. Dev. 69, 169–181.

Bouillet, P., Chazaud, C., Oulad-Abdelghani, M., Dolle, P., Chambon, P., 1995. Sequence and expression pattern of the *Stra7* (*Gbx-2*) homeobox-containing gene induced by retinoic acid in P19 embryonal carcinoma cells. Dev. Dyn. 204, 372–382.

Briscoe, J., Pierani, A., Jessell, T.M., Ericson, J., 2000. A homeodomain protein code specifies progenitor cell identity and neuronal fate in the ventral neural tube. Cell 101, 435–445.

Bulfone, A., Kim, H.J., Puelles, L., Porteus, M.H., Grippo, J.F., Rubenstein, J.L., 1993a. The mouse *Dlx-2* (*Tes-1*) gene is expressed in spatially restricted domains of the forebrain, face and limbs in midgestation mouse embryos. Mech. Dev. 40, 129–140.

Bulfone, A., Puelles, L., Porteus, M.H., Frohman, M.A., Martin, G.R., Rubenstein, J.L., 1993b. Spatially restricted expression of *Dlx-1*, *Dlx-2* (*Tes-1*), *Gbx-2*, and *Wnt-3* in the embryonic day 12.5 mouse forebrain defines potential transverse and longitudinal segmental boundaries. J. Neurosci. 13, 3155–3172.

Casarosa, S., Fode, C., Guillemot, F., 1999. Mash1 regulates neurogenesis in the ventral telencephalon. Development 126, 525–534.

Cavodeassi, F., Modolell, J., Gomez-Skarmeta, J.L., 2001. The *Iroquois* family of genes: from body building to neural patterning. Development 128, 2847–2855.

Cereghini, S., Ott, M.O., Power, S., Maury, M., 1992. Expression patterns of vHNF1 and HNF1 homeoproteins in early postimplantation embryos suggest distinct and sequential developmental roles. Development 116, 783–797.

Chiang, C., Litingtung, Y., Lee, E., Young, K.E., Corden, J.L., Westphal, H., Beachy, P.A., 1996. Cyclopia and defective axial patterning in mice lacking *Sonic hedgehog* gene function. Nature 383, 407–413.

Costantini, D.L., Arruda, E.P., Agarwal, P., Kim, K.H., Zhu, Y., Zhu, W., Lebel, M., Cheng, C.W., Park, C.Y., Pierce, S.A., Guerchicoff, A., Pollevick, G.D., Chan, T.Y., Kabir, M.G., Cheng, S.H., Husain, M., Antzelevitch, C., Srivastava, D., Gross, G.J., Hui, C.C., Backx, P.H., Bruneau, B.G., 2005. The homeodomain transcription factor *Irx5* establishes the mouse cardiac ventricular repolarization gradient. Cell 123, 347–358.

Couly, G., Creuzet, S., Bennaceur, S., Vincent, C., Le Douarin, N.M., 2002. Interactions between Hox-negative cephalic neural crest cells and the foregut endoderm in patterning the facial skeleton in the vertebrate head. Development 129, 1061–1073.

Creuzet, S., Schuler, B., Couly, G., Le Douarin, N.M., 2004. Reciprocal relationships between *Fgf8* and neural crest cells in facial and forebrain development. Proc. Natl. Acad. Sci. U. S. A. 101, 4843–4847.

Crossley, P.H., Martin, G.R., 1995. The mouse *Fgf8* gene encodes a family of polypeptides and is expressed in regions that direct outgrowth and patterning in the developing embryo. Development 121, 439–451.

Dattani, M.T., Martinez-Barbera, J.P., Thomas, P.Q., Brickman, J.M., Gupta, R., Martensson, I.L., Toresson, H., Fox, M., Wales, J.K., Hindmarsh, P.C., Krauss, S., Beddington, R.S., Robinson, I.C., 1998. Mutations in the homeobox gene *HESX1/Hesx1* associated with septo-optic dysplasia in human and mouse. Nat. Genet. 19, 125–133.

Davis, C.A., Joyner, A.L., 1988. Expression patterns of the homeobox-containing genes *En-1* and *En-2* and the proto-oncogene *int-1* diverge during mouse development. Genes Dev. 2, 1736–1744.

Depew, M.J., Tucker, A.S., Sharpe, P.T., 2002. Craniofacial development. In: Rossant, J., Tam, P.P. (Eds.), Mouse Development: Patterning, Morphogenesis, and Organogenesis. Academic Press, San Diego, pp. 421–498.

Echelard, Y., Epstein, D.J., St-Jacques, B., Shen, L., Mohler, J., McMahon, J.A., McMahon, A.P., 1993. Sonic hedgehog, a member of a family of putative signaling molecules, is implicated in the regulation of CNS polarity. Cell 75, 1417–1430.

Ericson, J., Muhr, J., Placzek, M., Lints, T., Jessell, T.M., Edlund, T., 1995. Sonic hedgehog induces the differentiation of ventral forebrain neurons: a

common signal for ventral patterning within the neural tube. Cell 81, 747–756.
Gomez-Skarmeta, J.L., Modolell, J., 2002. *Iroquois* genes: genomic organization and function in vertebrate neural development. Curr. Opin. Genet. Dev. 12, 403–408.
Götz, K., Briscoe, J., Rüther, U., 2005. Homozygous *Ft* embryos are affected in floor plate maintenance and ventral neural tube patterning. Dev. Dyn. 233, 623–630.
Grotewold, L., Rüther, U., 2002. The *Fused toes* (*Ft*) mouse mutation causes anteroposterior and dorsoventral polydactyly. Dev. Biol. 251, 129–141.
Heymer, J., Rüther, U., 1999. Syndactyly of *Ft*/+ mice correlates with an imbalance in *bmp4* and *fgf8* expression. Mech. Dev. 88, 173–181.
Heymer, J., Kuehn, M., Rüther, U., 1997. The expression pattern of nodal and lefty in the mouse mutant *Ft* suggests a function in the establishment of handedness. Mech. Dev. 66, 5–11.
Houweling, A.C., Dildrop, R., Peters, T., Mummenhoff, J., Moorman, A.F., Ruther, U., Christoffels, V.M., 2001. Gene and cluster-specific expression of the *Iroquois* family members during mouse development. Mech. Dev. 107, 169–174.
Itoh, M., Kudoh, T., Dedekian, M., Kim, C.H., Chitnis, A.B., 2002. A role for *iro1* and *iro7* in the establishment of an anteroposterior compartment of the ectoderm adjacent to the midbrain–hindbrain boundary. Development 129, 2317–2327.
Kiecker, C., Lumsden, A., 2005. Compartments and their boundaries in vertebrate brain development. Nat. Rev., Neurosci. 6, 553–564.
Kobayashi, D., Kobayashi, M., Matsumoto, K., Ogura, T., Nakafuku, M., Shimamura, K., 2002. Early subdivisions in the neural plate define distinct competence for inductive signals. Development 129, 83–93.
Kuhlbrodt, K., Herbarth, B., Sock, E., Hermans-Borgmeyer, I., Wegner, M., 1998. *Sox10*, a novel transcriptional modulator in glial cells. J. Neurosci. 18, 237–250.
Kuschel, S., Rüther, U., Theil, T., 2003. A disrupted balance between *Bmp/Wnt* and *Fgf* signaling underlies the ventralization of the *Gli3* mutant telencephalon. Dev. Biol. 260, 484–495.
Lazzaro, D., Price, M., de Felice, M., Di Lauro, R., 1991. The transcription factor TTF-1 is expressed at the onset of thyroid and lung morphogenesis and in restricted regions of the foetal brain. Development 113, 1093–1104.
Lecaudey, V., Anselme, I., Rosa, F., Schneider-Maunoury, S., 2004. The zebrafish *Iroquois* gene *iro7* positions the r4/r5 boundary and controls neurogenesis in the rostral hindbrain. Development 131, 3121–3131.
Le Douarin, N., Kalcheim, C., 1999. The Neural Crest. Cambridge Univ. Press, New York.
Lesche, R., Peetz, A., van der Hoeven, F., Rüther, U., 1997. *Ft1*, a novel gene related to ubiquitin-conjugating enzymes, is deleted in the *Fused toes* mouse mutation. Mamm. Genome 8, 879–883.
Ma, Q., Kintner, C., Anderson, D.J., 1996. Identification of *neurogenin*, a vertebrate neuronal determination gene. Cell 87, 43–52.
Maden, M., Horton, C., Graham, A., Leonard, L., Pizzey, J., Siegenthaler, G., Lumsden, A., Eriksson, U., 1992. Domains of cellular retinoic acid-binding protein I (CRABP I) expression in the hindbrain and neural crest of the mouse embryo. Mech. Dev. 37, 13–23.
Marcucio, R.S., Cordero, D.R., Hu, D., Helms, J.A., 2005. Molecular interactions coordinating the development of the forebrain and face. Dev. Biol. 284, 48–61.
Marin, O., Rubenstein, J.L., 2002. Patterning, regionalization, and cell differentiation in the forebrain. In: Rossant, J., Tam, P.P. (Eds.), Mouse Development: Patterning, Morphogenesis and Organogenesis. Academic Press, San Diego, pp. 75–106.
Matsumoto, K., Nishihara, S., Kamimura, M., Shiraishi, T., Otoguro, T., Uehara, M., Maeda, Y., Ogura, K., Lumsden, A., Ogura, T., 2004. The prepattern transcription factor *Irx2*, a target of the FGF8/MAP kinase cascade, is involved in cerebellum formation. Nat. Neurosci. 7, 605–612.
Muenke, M., Cohen Jr., M.M., 2000. Genetic approaches to understanding brain development: holoprosencephaly as a model. Ment. Retard. Dev. Disabil. Res. Rev. 6, 15–21.
Novitch, B.G., Chen, A.I., Jessell, T.M., 2001. Coordinate regulation of motor neuron subtype identity and pan-neuronal properties by the bHLH repressor Olig2. Neuron 31, 773–789.
Oliver, G., Mailhos, A., Wehr, R., Copeland, N.G., Jenkins, N.A., Gruss, P., 1995. *Six3*, a murine homologue of the *sine oculis* gene, demarcates the most anterior border of the developing neural plate and is expressed during eye development. Development 121, 4045–4055.
Park, H.L., Bai, C., Platt, K.A., Matise, M.P., Beeghly, A., Hui, C.C., Nakashima, M., Joyner, A.L., 2000. Mouse *Gli1* mutants are viable but have defects in SHH signaling in combination with a *Gli2* mutation. Development 127, 1593–1605.
Peters, T., Ausmeier, K., Rüther, U., 1999. Cloning of *Fatso* (*Fto*), a novel gene deleted by the *Fused toes* (*Ft*) mouse mutation. Mamm. Genome 10, 983–986.
Peters, T., Ausmeier, K., Dildrop, R., Ruther, U., 2002. The mouse *Fused toes* (*Ft*) mutation is the result of a 1.6-Mb deletion including the entire *Iroquois B* gene cluster. Mamm. Genome 13, 186–188.
Qiu, M., Bulfone, A., Ghattas, I., Meneses, J.J., Christensen, L., Sharpe, P.T., Presley, R., Pedersen, R.A., Rubenstein, J.L., 1997. Role of the *Dlx* homeobox genes in proximodistal patterning of the branchial arches: mutations of *Dlx-1*, *Dlx-2*, and *Dlx-1* and *-2* alter morphogenesis of proximal skeletal and soft tissue structures derived from the first and second arches. Dev. Biol. 185, 165–184.
Rhinn, M., Brand, M., 2001. The midbrain–hindbrain boundary organizer. Curr. Opin. Neurobiol. 11, 34–42.
Robb, L., Tam, P.P., 2004. Gastrula organiser and embryonic patterning in the mouse. Semin. Cell Dev. Biol. 15, 543–554.
Ruberte, E., Dolle, P., Chambon, P., Morriss-Kay, G., 1991. Retinoic acid receptors and cellular retinoid binding proteins: II. Their differential pattern of transcription during early morphogenesis in mouse embryos. Development 111, 45–60.
Schneider, R.A., Hu, D., Rubenstein, J.L., Maden, M., Helms, J.A., 2001. Local retinoid signaling coordinates forebrain and facial morphogenesis by maintaining *FGF8* and *SHH*. Development 128, 2755–2767.
Shimamura, K., Rubenstein, J.L., 1997. Inductive interactions direct early regionalization of the mouse forebrain. Development 124, 2709–2718.
Shimamura, K., Hartigan, D.J., Martinez, S., Puelles, L., Rubenstein, J.L., 1995. Longitudinal organization of the anterior neural plate and neural tube. Development 121, 3923–3933.
Shimamura, K., Martinez, S., Puelles, L., Rubenstein, J.L., 1997. Patterns of gene expression in the neural plate and neural tube subdivide the embryonic forebrain into transverse and longitudinal domains. Dev. Neurosci. 19, 88–96.
Shimogori, T., Banuchi, V., Ng, H.Y., Strauss, J.B., Grove, E.A., 2004. Embryonic signaling centers expressing BMP, WNT and FGF proteins interact to pattern the cerebral cortex. Development 131, 5639–5647.
Shinozaki, K., Yoshida, M., Nakamura, M., Aizawa, S., Suda, Y., 2004. *Emx1* and *Emx2* cooperate in initial phase of archipallium development. Mech. Dev. 121, 475–489.
Simeone, A., Acampora, D., Gulisano, M., Stornaiuolo, A., Boncinelli, E., 1992. Nested expression domains of four homeobox genes in developing rostral brain. Nature 358, 687–690.
Simeone, A., Acampora, D., Mallamaci, A., Stornaiuolo, A., D'Apice, M.R., Nigro, V., Boncinelli, E., 1993. A vertebrate gene related to orthodenticle contains a homeodomain of the bicoid class and demarcates anterior neuroectoderm in the gastrulating mouse embryo. EMBO J. 12, 2735–2747.
Simeone, A., Acampora, D., Pannese, M., D'Esposito, M., Stornaiuolo, A., Gulisano, M., Mallamaci, A., Kastury, K., Druck, T., Huebner, K., et al., 1994. Cloning and characterization of two members of the vertebrate *Dlx* gene family. Proc. Natl. Acad. Sci. U. S. A. 91, 2250–2254.
Storm, E.E., Rubenstein, J.L., Martin, G.R., 2003. Dosage of *Fgf8* determines whether cell survival is positively or negatively regulated in the developing forebrain. Proc. Natl. Acad. Sci. U. S. A. 100, 1757–1762.
Storm, E.E., Garel, S., Borello, U., Hebert, J.M., Martinez, S., McConnell, S.K., Martin, G.R., Rubenstein, J.L., 2006. Dose-dependent functions of *Fgf8* in regulating telencephalic patterning centers. Development 133, 1831–1844.
Stoykova, A., Gruss, P., 1994. Roles of *Pax*-genes in developing and adult brain as suggested by expression patterns. J. Neurosci. 14, 1395–1412.
Theil, T., Alvarez-Bolado, G., Walter, A., Ruther, U., 1999. *Gli3* is required for *Emx* gene expression during dorsal telencephalon development. Development 126, 3561–3571.

Thomas, P., Beddington, R., 1996. Anterior primitive endoderm may be responsible for patterning the anterior neural plate in the mouse embryo. Curr. Biol. 6, 1487–1496.

Tole, S., Ragsdale, C.W., Grove, E.A., 2000. Dorsoventral patterning of the telencephalon is disrupted in the mouse mutant *extra-toes(J)*. Dev. Biol. 217, 254–265.

van der Hoeven, F., Schimmang, T., Volkmann, A., Mattei, M.G., Kyewski, B., Rüther, U., 1994. Programmed cell death is affected in the novel mouse mutant *Fused toes* (*Ft*). Development 120, 2601–2607.

Wilkinson, D.G., 1992. Whole-mount in situ hybridisation of vertebrate embryos. In: Wilkinson, D.G. (Ed.), In Situ Hybridisation: A Practical Approach. IRL Press, Oxford, pp. 75–83.

Wilkinson, D.G., Bailes, J.A., McMahon, A.P., 1987. Expression of the proto-oncogene *int-1* is restricted to specific neural cells in the developing mouse embryo. Cell 50, 79–88.

Wilkinson, D.G., Bhatt, S., Cook, M., Boncinelli, E., Krumlauf, R., 1989. Segmental expression of *Hox-2* homoeobox-containing genes in the developing mouse hindbrain. Nature 341, 405–409.

Wilson, S.W., Houart, C., 2004. Early steps in the development of the forebrain. Dev. Cell 6, 167–181.